Thermomechanical Behavior of Polymer/Layered Silicate Clay Nanocomposites Based on Unmodified Low Density Polyethylene

K. Grigoriadi,[1] A. Giannakas,[2] A. Ladavos,[2] N.-M. Barkoula[1]
[1] *Department of Materials Science and Engineering, University of Ioannina, Ioannina 45110, Greece*

[2] *School of Natural Resources and Enterprise Management, University of Western Greece, Agrinio 30100, Greece*

The purpose of this study was to investigate the effect of filler content and aspect ratio on the thermomechanical behavior of unmodified low density polyethylene (LDPE)-based layered silicate clay nanocomposites. LDPE-based nanocomposites, without any polymer modification and with two kinds of clays, one with low aspect ratio (i.e., synthetic laponite -Lp) and another with high aspect ratio (i.e., montmorillonite) were prepared and characterized using dynamic mechanical analysis (DMA). Organosilicates were added at 2, 5 and 10 wt%, respectively. X-ray diffraction (XRD) analysis was performed on composites obtained by dispersing the organosilicates in unmodified LDPE. The LPDE reinforced with organo-montmorillonite (OMt) had better performance in the whole temperature range than those with organo-laponite (OLp). It was concluded that the relatively high aspect ratio OMt can induce superior dynamic mechanical properties to the LDPE polymer compared to lower aspect ratio OLp. This was linked to the higher active surface area and preferential orientation of longer platelets resulting in higher mechanical enhancement. This behavior was more pronounced up to filler contents of 5 wt%. Further increase of the filler content led to more conventional composites, which hindered the reinforcing ability of the silicates. POLYM. ENG. SCI., 00:000–000, 2012. © 2012 Society of Plastics Engineers

INTRODUCTION

Polymer/layered silicate (PLS) nanocomposites have recently become quite important for both industry and academia because of their superior performance compared to virgin polymer or conventional micro and macrocomposites. Improvements of the elastic moduli, strength, heat resistance, barrier properties, and flame retardancy have been reported in the open literature [1–6]. Layered silicate clays are good candidates as reinforcement in the design of nanocomposites due to their lamellar structure that have high inplane strength and stiffness and a high aspect ratio (>50). Smectite clays (e.g. montmorillonite), is the main choice for PLS nanocomposites [7, 8]. The key reasons are their rich intercalation chemistry, which allows them to be chemically modified and become compatible with organic polymers for dispersal on a nanometer scale, and their relative low costs [7, 9–11]. Clay based polymer nanocomposites can exhibit two extreme morphologies, i.e. intercalated and exfoliated [2–4, 6, 12–14]. In the intercalated structure the polymer chains penetrate in between the silicate layers. When the clay layers disperse as single platelets throughout the polymer matrix exfoliated nanocomposites are being obtained [2–4, 6, 12–14]. It is possible that during composites preparation none of these morphologies is achieved and then conventional composites are obtained which contain clay particles with micron-scale dimensions. Depending on the state of clays huge differences are seen in the interfacial area per unit volume. High interfacial area leads to enhanced interaction between anisotropic clay platelets and the polymer, and is the cause for the notable differences in the physical, mechanical and melt-phase properties between nanocomposites and conventional composites [13]. In order to favor these morphologies, clay must be ion-exchanged to reduce the cohesive forces between clay platelets. Next to that, existence of polar groups in both the polymer and the clay layers favor these interactions. In the case of non-polar polymers like polyethylene (PE), polypropylene (PP) there is very little or no interaction between the polar clay layers and the non-polar polymer [3, 6, 13–16]. Various authors [4, 13, 14, 16–21] reported on the dispersion of clay platelets in polyolefins by addition of a compatibilizer such as maleated polypropylene or maleated polyethylene. Another strategy is based on the intercalative polymerization of the monomer. In this technique,

Correspondence to: N.-M. Barkoula; e-mail: nbarkoul@cc.uoi.gr
Contract grant sponsor: European Union-European Regional Development Fund and Greek Ministry of Education; contract grant number: 09ΣΥΝ-42-831.
DOI 10.1002/pen.23264
Published online in Wiley Online Library (wileyonlinelibrary.com).
© 2012 Society of Plastics Engineers

the monomer is intercalated within the silicate layers together with the polymerization catalyst [22–26].

PE film is widely used in packaging industries because of its exceptional properties, such as light weight, low cost, and easy processability. The synthesis of LDPE/inorganic nanocomposites with improved properties, such as mechanical and barrier properties, is expected to further boost its use in that direction. Many studies have been reported on the preparation and characterization of high density polyethylene (HDPE)/clay nanocomposites [3, 6, 27, 28]. The achievement of LDPE nanocomposite structures with highly dispersed inorganic nanoparticles is much more difficult than HDPE ones because of the branched macromolecules (in LDPE), which hinder the penetration of the polymer chains into the clay galleries [29]. Modified LDPE/ clay nanocomposites have been achieved and studied in the past [6, 20, 21, 30, 31], however very limited data are available on unmodified LDPE/ clay nanocomposites [15, 29].

Thermomechanical properties are of key importance for the applicability of LDPE/inorganic nanocomposites. Previous studies report that the formation of a superstructure of the dispersed layers in the polymer matrix governs the linear viscoelastic properties of layered-silicate-based nanocomposites [32–34]. Studies on LDPE with compatibilizer and clays as reinforcement revealed that the dynamic viscoelastic properties of composite are strongly dependent on the intercalation of polymer and exhibited dramatically change with altering intercalation conditions [31]. It has been reported that not only the dispersion but also the orientation of the clay platelets could affect the viscoelastic properties of the nanocomposites [33]. The aspect ratio of the clays has been also suggested to be of key importance for both the static mechanical properties of HDPE nanocomposites as well as storage moduli and complex viscosity [2, 3, 19].

Based on the above, the current study aims in experimentally determining the thermomechanical properties of LDPE-based nanocomposites, without any polymer modification and with two kinds of layered silicates (clays), one with low aspect ratio (i.e., synthetic laponite) and another with high aspect ratio (i.e., montmorillonite) using dynamic mechanical analysis (DMA). X-ray diffraction (XRD) gives quantitative data on the dispersion of the clay platelets. Since this is important for the interpretation of the DMA results, XRD analysis has been used to determine the structure of the obtained PLS nanocomposites.

EXPERIMENTAL

Two layered silicates clays were used in this work, i.e. (i) Lp, obtained from Southern Clay Products, with cation exchange capacity (CEC) 50 meq/100 g of clay (its surface modification is described later) and (ii) OMt NANOMER −I.44P produced by Nanocor Company and supplied by Aldrich (Milwaukee, WI). Surface modification of the synthetic laponite was carried out using the same surfactant as that used by Nanocor in NANOMER-I.44P organoclay, namely Arquad 2HT-75, produced by Akzo and supplied by Fluka (Buchs SG, Switzerland). A 1 wt % solution of surfactant in warm water was prepared and added dropwise to a 1 wt % Lp suspension. The obtained mixture was stirred vigorously for 24 h at 70°C. The amount of the surfactant added was equivalent to 1.5× the CEC of Lp. The resulting samples were washed four times with deionized water and once with ethanol to remove the excess of surfactant and dried in a vacuum oven at 40°C. The Lp had a low aspect ratio (20–30) and the montmorillonite had high aspect ratio (100–200). The polyethylene used for the nanocomposites preparation was LDPE supplied by Aldrich, with Melt Index = 25 g/10 min (190°C/2.16 kg) and density 0.915 g cm^{-3}.

LDPE-OLp and LDPE-OMt composites with 2, 5, and 10 wt% organosilicate loadings have been obtained by melting at 180°C in an oven, composites prepared via the solution method [29]. The solution method involved the dilution of appropriate amounts of LDPE in CCl_4 at 85°C and mixing the solution with 1.5× CEC- OLp or OMt. The mixtures remained for 24 h under stirring at 85°C. The final composites were received after solvent evaporation. For better homogenization during melting, periodical mechanical stirring (out of the oven) using a micromixer (IKA-WERKE model DI 25) with stirring speed 8000 rpm was applied.

The dynamic mechanical behavior of the LDPE and LDPE-nanocomposites was measured on a NETZSCH DMA 242C apparatus. Dynamic temperature spectra of the samples were obtained in tensile mode at a vibration frequency of 1 Hz, at temperatures ranging from −120 to 90°C, at a rate of 2°C/min. Cooling was achieved using liquid N_2. The amplitude of the deformation was 40 μm, which was small enough to ensure a linear viscoelastic response from the samples.

Samples of layered organosilicates for XRD analysis were prepared by spreading about 1 mL of their water suspension (10 mg/mL) on glass slides. The water was evaporated (at RT) before the X-ray measurements. The XRD measurements were performed on a D8 Advanced Bruker diffractometer with CuKa radiation (λ = 1.5418 Å) and the basal spacing of the samples was estimated from the *d*-spacing of the 001 reflection. XRD analyses of polymer nanocomposites took place on films prepared using a hydraulic press with heated platens, in the same diffractometer.

RESULTS AND DISCUSSION

As aforementioned, the thermomechanical properties of LDPE/inorganic nanocomposites are of key importance for their applicability, especially in the packaging industry where variations in storage/operational temperatures are very common. In Fig. 1 the storage modulus of the LDPE, LDPE/OLp, and LDPE/OMt modified nanocomposites with various organoclay loadings (2–10 wt %) is

 DOI 10.1002/pen

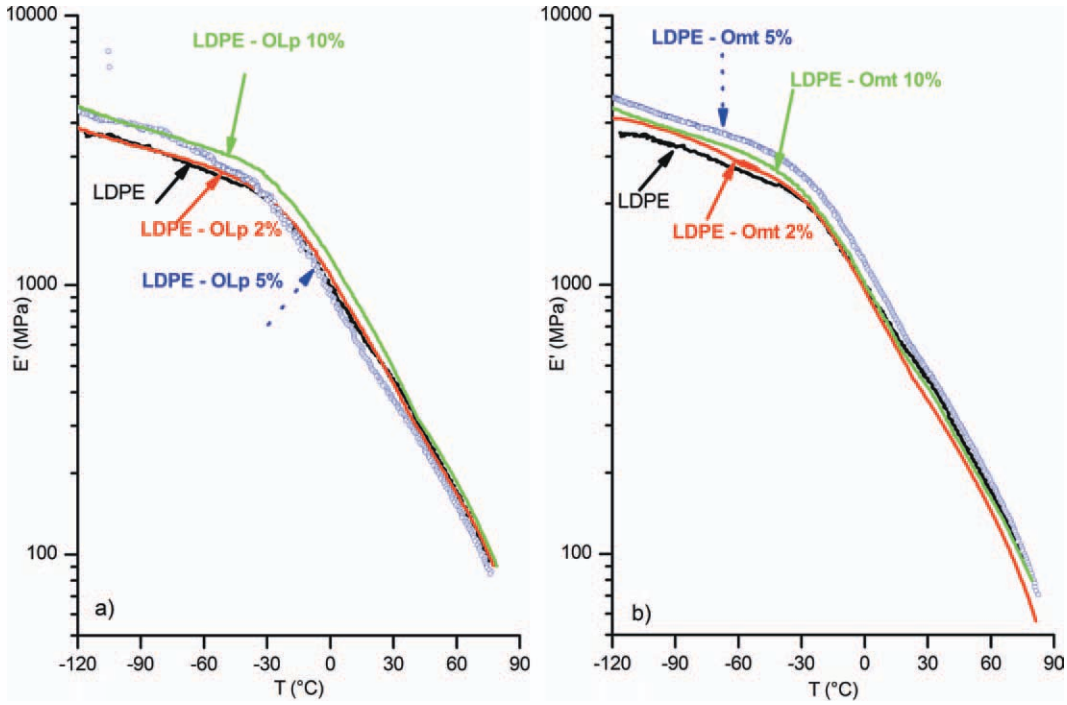

FIG. 1. Storage modulus E' as a function of temperature of unmodified, OLp (a) and OMt (b) modified nanocomposites with various clay loadings (2–10 wt%). [Color figure can be viewed in the online issue, which is available at wileyonlinelibrary.com.]

plotted against temperature. As can be seen from this graph the tendency is a significant increase (note the logarithmic scale) of the storage modulus of the polymer/clay nanocomposites compared to that of the unmodified LPDE especially at temperatures below ambient (at $\sim -20^{\circ}$C). In the case of OLp modified materials there is a direct relation between the OLp concentration and the increase in stiffness. More specifically, the OLp nanocomposites with 2 wt% reinforcement present similar behavior with that of the unmodified system, while as the OLp concentration increases the increase in the storage modulus is more obvious initially at low temperatures (below -20°C) and at 10 wt% OLp concentration at the whole temperature range. Maximum improvement of about 40% is observed at 10 wt% OLp concentration (calculated at -120°C). OMt based nanocomposites present improved storage modulus at low temperatures (below -20°C) while at higher temperatures a small deterioration is being observed. This holds for all OMt concentrations except of 5 wt% reinforcement. OMt addition at 5 wt% concentration offers the highest reinforcing ability at the whole temperature range, which is $\sim$55% (calculated at -120°C). A further OMt addition (10 wt %) leads to small decrease of the stiffness, resulting into values similar to those of the LPDE- OLp 10% nanocomposites. It is interesting to note that LPDE-OMt 5% has better performance in the whole temperature range than LPDE-OLp 10% nanocomposites. In a recent publication on the static properties of LDPE nanoclays, it was shown that the mechanical properties were superior for the LDPE-OMt composites, whereas OLp offered improved properties with lower however reinforcing ability [29], which is in agreement with the dynamic mechanical response presented here. As observed for both OLp and OMt nanocomposites the reinforcing ability of the nanoclays was linked to their concentration as well as to a specific temperature (-20°C) below which the reinforcing ability of the nanoclays was more obvious. At high temperatures (higher than -20°C) due to the increased mobility of the polymer chains it is observed that nanoclays still offer some reinforcing to LDPE only when a sufficient amount is present. This temperature is related to the β-relaxation of the LDPE and its role will be discussed in detail in the next paragraph.

Figure 2 presents the loss modulus of the materials under investigation as a function of temperature. In the unmodified LDPE three relaxations are normally observed, identified as α, β, and γ in order of decreasing temperature. The α-relaxation is normally observed between 30°C and the melting point, and intensifies with increasing crystallinity, the β-relaxation between -55°C and 25°C, and the γ-relaxation between -145°C and -95°C [35]. In Fig. 2, one peak can be observed at approximately -20°C, associated with the β-relaxation of LDPE. Due to the fact that the DMA measurements started at -120°C it is not possible to draw any conclusion regarding the effect of OMt/OLp addition on the γ-relaxation. The γ-relaxation is generally accepted as the glass transition temperature (T_g) of PE. Regarding the β-relaxation, the addition of OMt seems to result in a

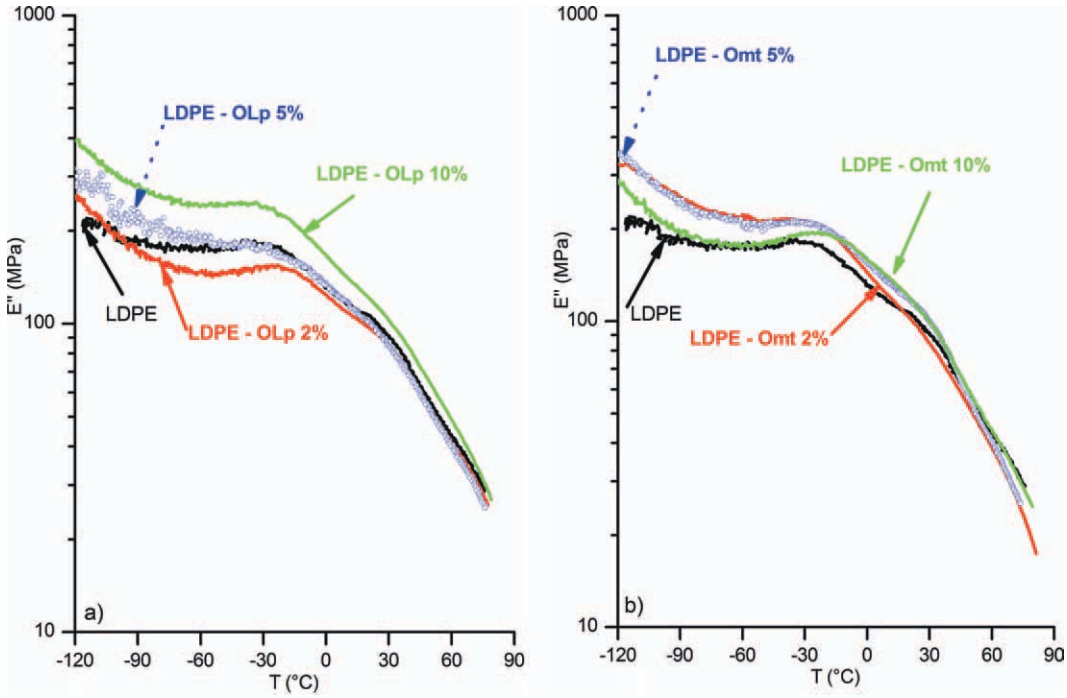

FIG. 2. Loss modulus E'' as a function of temperature of unmodified, OLp (a) and OMt (b) modified polymer nanocomposites with various organoclay loadings (2–10 wt%). [Color figure can be viewed in the online issue, which is available at wileyonlinelibrary.com.]

very small shift of the peak to higher values in the case of 10 wt% content, while OLp did not affect significantly the peak. Based on previous studies on PE the β-relaxation is believed to offer information about the chain architecture of PE. One of the suggestions is that this relaxation is due to motion in the amorphous phase near branch points [36]. It can be proposed that the existence of higher aspect ratio clay platelets in case of LDPE/OMt nanocomposites resulted in higher degree of branching of the amorphous phase and therefore in a small increase in the activation temperature of such movements. Finally, α transition is almost absent and can be hardly distinguished in the unmodified LDPE. Previews studies revealed that α transition of LDPE is small and broad [37] due to the low crystallinity of LDPE. The existence of nanoparticles has been identified in the past as an influencing parameter on crystallization kinetics since they act as nucleating agents facilitating the heterogeneous crystallization process. It was suggested by Gopakumar et al. [13] that due to restrictions in polymer chain mobility through association with exfoliated platelets, a significant reduction in the degree of crystallinity is observed, which can negate the reinforcing capability of the nanoclays. A recent publication on the same materials as those under investigation [29] discussed the effect of OLp and OMt addition on the crystallization of LDPE nanocomposites. Based on the DSC results, it was suggested that LDPE/OLp nanocomposites revealed a gradual increase in the crystallization temperatures (T_c) from 100.2°C to 102.6°C with increasing OLp content, whereas for nanocomposites prepared using OMt, T_c values remained constant and similar to those of the neat LDPE [29]. The observed increase of the T_c with increasing clay content was attributed to the nucleation controlled polymer crystallization, where the presence of small silicate layers induced the formation of nuclei and crystals which started growing at higher temperatures. In the case of the OMt-based composites, the OMt clay platelets with relatively large aspect ratio did not induce the nucleation-controlled polymer crystallization [29]. The clay addition had a marginal effect on the crystallization kinetics, and hence cannot be detected on the DMA curves presented in Figs. 1 and 2. Finally it can be seen that as in case of the storage modulus the addition of OLp/OMt led to an increase of the loss modulus at temperatures below ambient, however this is less obvious at high temperatures.

Increased stiffness/storage modulus results normally to a decrease in the loss energy and thus contribute toward a decrease in the damping of a material. In other words, if the clay acts as reinforcement a decrease in the tan δ curve will be observed. In Fig. 3 the tan δ of the unmodified polymer and polymer/clay nanocomposites is being plotted. The addition of OLp/OMt led to lower damping at temperatures below ambient and higher damping at high temperatures. Some discrepancies from this tendency are found at 10 wt% OLp and 2 wt% OMt, where increased damping at low temperatures is being observed. The decrease of the damping character of the chains at low temperatures upon addition of clay layers is because of the fact that while both E' and E'' increase, the elastic-

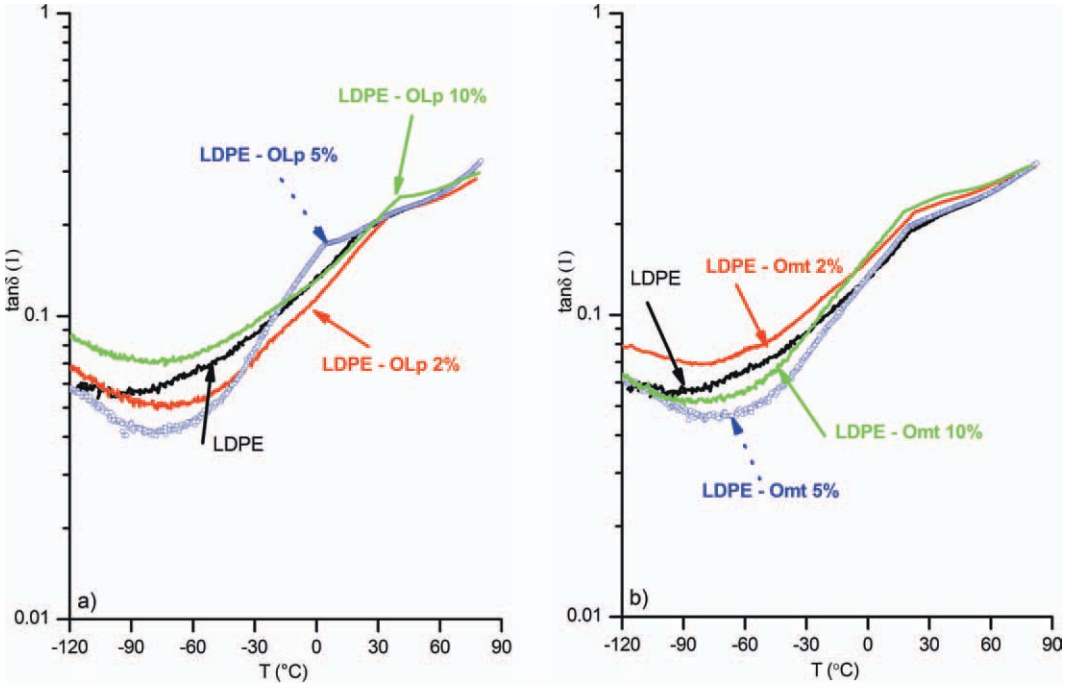

FIG. 3. Loss factor (tan δ) as a function of temperature of unmodified, OLp (a) and OMt (b) modified nanocomposites with various organoclay loadings (2–10 wt%). [Color figure can be viewed in the online issue, which is available at wileyonlinelibrary.com.]

ity characteristics of the nanocomposite increase more drastically compared to the plasticity characteristics, therefore the decrease in the tan δ ratio. In general, the decrease in the tan δ ratio with increasing intercalated clay platelet basal plane orientation reflects the increasing reinforcement ability of the clay layers. Due to the existence of crystalline regions, amorphous regions and branching regions, chains activation occurs at different temperatures. This explains why the transitions in the E'' and in the tan δ curves are not sharp. Finally it can be observed that clear peaks on the tan δ curves are present around ambient temperature in both OLp and OMt nanocomposite systems. In the case of the OLp nanocomposites the peak is shifting depending on the OLp concentration, while in the case of the OMt nanocomposite it remains almost constant at around 30°C. This could be linked to the aforementioned effect of nanoclays on the crystallization kinetics, and hence on the α relaxation documented in the case of OLp nanocomposites, which is absent in the case of the OMt systems.

The obtained results from the DMA tests compare quite well at temperatures below −20°C with those published on a cross-linked LDPE clay nanocomposite [38]. As aforementioned this temperature was identified as the β-relaxation of the LDPE nanocomposites and it was suggested that this relaxation is due to motion in the amorphous phase near branch points [36]. The addition of clays resulted in an increased amount of branch points, which were also favored from the branching nature of LDPE. At higher temperatures an increased mobility is observed in the aforementioned regions, which results in lowering the reinforcing potential of the nano-clays. This can be limited if crosslinking is of instance present as described by Rezanejad and Kokabi [38].

In order to understand the reinforcing efficiency of the clay platelets the morphology of the obtained nanocomposites should be considered and discussed. XRD patterns of the OLp and the OLp-based nanocomposites are shown in Fig. 4a. As can be seen in this figure, the XRD peak that corresponds to clay basal spacing becomes very broad and its intensity is quite low that the peak almost diminishes. Figure 4b presents the XRD patterns of the OMt and the OMt-based nanocomposites. In the case of the LDPE/OMt composites, the XRD peaks that correspond to clay basal spacing are still present but are shifted to lower angles (i.e., higher d-spacing values). Based on the patterns presented in Fig. 4a and b it can be suggested that nanocomposite structure has occurred for both the OLp- and OMt-based composites, especially at low filler content. In the case of the OLp-based nanocomposites the fact that the clay peak almost disappears may be a suggestion that an exfoliated or partially exfoliated structure has been obtained to a certain extent. On the other hand the shift of the clay basal spacing to lower angles in the case of the LDPE/OMt composites is indicative of an intercalated structure where the polymer chains are incorporated between the silicate layers, increasing their gallery height but maintaining their layered stacking with alternating polymer/silicate layers [29]. The intensity of the clay peak is lower for the OMt-based nanocomposites at 2 wt% filler content. This is indicative that the lower the filler content the easier the separation of the clay platelets. These

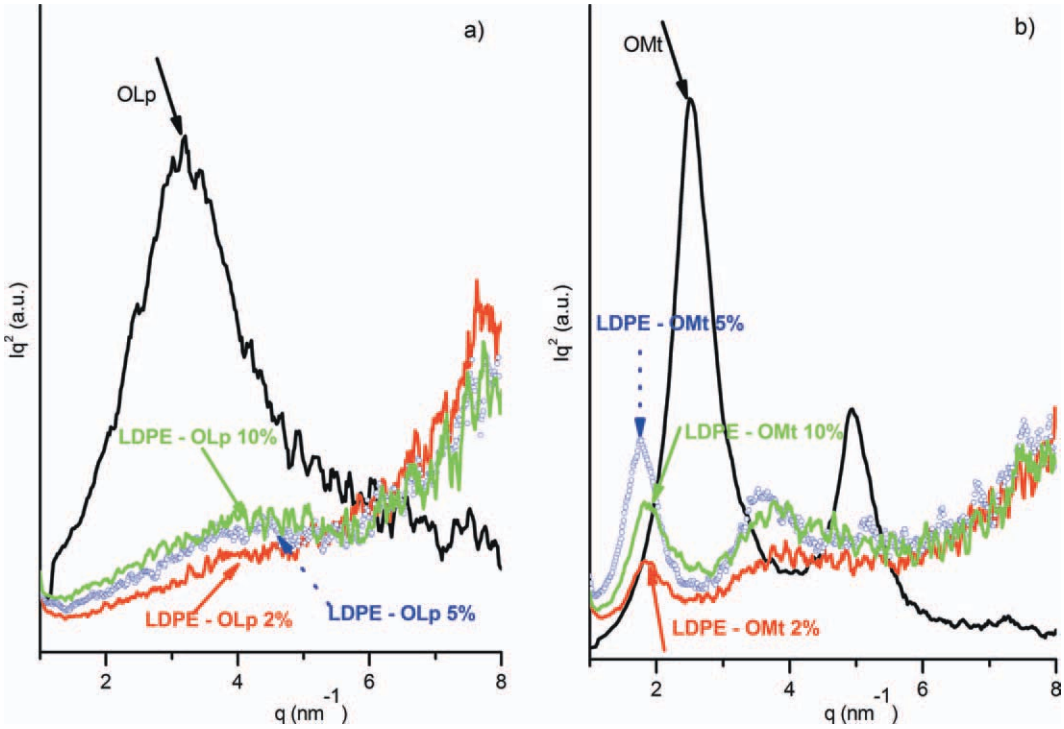

FIG. 4. XRD patterns of various LDPE/organosilicate composites prepared by OLp (a) and OMt (b) in the form of $Iq^2 = f(q)$, where I is the intensity and $q = 4\pi \sin \theta/\lambda$. The patterns of OLp and OMt samples are also shown for direct comparison. [Color figure can be viewed in the online issue, which is available at wileyonlinelibrary.com.]

findings are in line with previous observations from the same group on the same material [29] where low aspect ratio silicates (20–30) (OLp), favored the formation of exfoliated or partially exfoliated nanocomposite structure whereas silicates with high aspect ratio (100–200) like OMt preferred intercalated nanostructure formation.

One would expect that an exfoliated structure would offer higher reinforcing ability compared to a partially exfoliated or intercalated structure. When polymer enters into clay galleries, the nanocomposite is intercalated, but since a small amount of clay is used, a large amount of free polymer forms the reinforcement [39]. If the clay platelets are exfoliated in the polymer matrix, then the platelets themselves provide the reinforcement. If the clay stays in particle-form in the polymer matrix, the composite is conventional and the elastic modulus of the bulk clay mineral rather than that of the platelets is required for interpretation [39]. Nanoclays anchor at different positions in the matrix, thus restricting the movement of the polymer chains. An exfoliated structure results in higher amount of anchoring points compared to a partially exfoliated or intercalated structure. On the other hand the enhancement of storage modulus depends also on the aspect ratio of the dispersed clay layers. The active surface area between the filler and the matrix increases with the degree of exfoliation as well as with the aspect ratio and clay orientation.

The reinforcing efficiency of nanofillers has been estimated in the past using conventional composite theories [40–43]. Most of the composite theories correlate the modulus of the composite with the volume fraction as well as the aspect ratio of the filler [40, 43]. Since clay platelets are asymmetric the stiffness of the nanocomposite will depend on the degree of exfoliation/intercalation as well as the orientation of the clay basal plane to the testing direction. The prerequisite for the application of such models is the fillers to have platelet-like shape and their content to be low enough to avoid any agglomeration of the particles [40]. The most commonly used equations for fitting the modulus of polymer nanocomposites are the Halpin-Tsai [44] and the modified Halpin-Tsai equations [45]. The modified Halpin-Tsai equation incorporate an orientation factor (α) to account for the randomness of discontinuous nanotubes [45]. When the filler length is greater than the specimen thickness, the fillers assumed to be randomly oriented in two dimensions, i.e., the orientation factor $\alpha = 1/3$. When the filler length is much smaller than the thickness of the specimen, the fillers are assumed to be randomly oriented in three dimensions, i.e., the orientation factor $\alpha = 1/6$ [45].

An indirect way therefore to estimate the exfoliation/intercalation of the clays in nanocomposites examined here is to assume an ideal dispersion (perfectly exfoliated structure) and calculate the effective modulus. The comparison of the calculated modulus with the measured one can provide an indication of the degree of exfoliation/intercalation. In order to do so the modified Halpin-Tsai equations have been adapted. The mathematical expression of the modified Halpin-Tsai equation is as follows:

TABLE 1. Input parameters for the calculation of the composite's modulus based on *Eqs. 1* and *2*.

W_f (%)	W_m (%)	ρ_f (kg/m^3)	ρ_m (kg/m^3)	V_f (%)	V_m (%)	E_f (GPa)	E_m (GPa)	L/d OLp (1)	L/d OMt (1)
2	98	3067	920	0.01	0.99	176	3.5	30	200
5	95	3067	920	0.02	0.98	176	3.5	30	200
10	90	3067	920	0.03	0.97	176	3.5	30	200

Abbreviations: W_f, weight fraction of the filler; W_m, weight fraction of the matrix; ρ_f, density of the filler; ρ_m, density of the matrix.

$$E_c = \frac{1 + (2L/d)\eta v_f}{1 - \eta v_f} E_m \quad (1)$$

in which

$$\eta = \frac{\alpha(E_f/E_m) - 1}{\alpha(E_f/E_m) + 2L/d} \quad (2)$$

where E_c, E_f and E_m are the moduli of the composite, matrix and filler, respectively, v_f is the volume fraction of the filler, α is an orientation factor to account for the randomness of the filler, and L/d is the aspect ratio of the filler. The L/d parameter of clay particles in nanocomposites is conventionally considered as a measure of filler dispersion throughout the polymer matrix [46]. Since successful direct experimental measurements on montmorillonite or hectorite platelets are presently not found in the literature, an approach is to look at the elastic modulus of clays with the same or similar layer structure but without interlayer spacing [39]. An elastic modulus of 178 GPa and a density of 3067 kg/m^3 have already been adopted on the basis that muscovite has a similar structure to clay platelets [39]. The elastic modulus and density of the bulk clay is suggested to be 21 GPa and 2600 kg/m^3 [39], respectively. The input parameters for the calculation of the composite's modulus based on *Eqs 1* and *2* are presented in Table 1. An orientation factor $\alpha = 1/6$ was used in this study.

Based on these input parameters the effective storage modulus has been calculated and is presented in Table 2, assuming that clays are ideally dispersed in an exfoliated manner. Since clays are not viscoelastic materials, it is expected that their properties do not vary with temperature. For the LDPE the storage modulus has been taken at $-120°$C from the experimental data presented in Fig. 1. The measured storage modulus for LDPE-OMt and LDPE-OLp composites at 2, 5 and 10 wt% is presented for comparison in the last two columns of Table 2. The values have been taken again from Fig. 1 at temperatures of $-120°$C. Based on the data presented in Table 2, it can be said that the measured E' compare well with the calculated ones in the case of the OLp nanocomposites, supporting the XRD observations that a partially exfoliated/exfoliated structure has been achieved. In the case of the OMt nanocomposites a relatively good agreement can be found between the calculated and the measured values for 2 and 5 wt% contents. On the other hand the 10 wt% reinforcement provided values well behind the calculated ones for an exfoliated system. It seems that the addition of higher amount of clays hindered the ability of clay platelet dispersion and the obtained composites are more conventional as described previously [29]. The OMt based nanocomposites with 2 wt% and 5 wt% have slightly higher modulus compared to that of the OLp ones, which is because of the higher aspect ratio of the OMt clay. It can be suggested therefore that the relatively high aspect ratio OMt clay platelets can induce superior mechanical properties to the LDPE polymer compared to lower aspect ratio clay (OLp) even if they are not fully exfoliated/intercalated.

CONCLUSIONS

The aim of this paper was to investigate the thermomechanical properties of LDPE-based nanocomposites, without any polymer modification and with two kinds of layered silicates (clays), one with low aspect ratio (i.e., synthetic laponite) and another with high aspect ratio (i.e., montmorillonite) using DMA. Based on the thermomechanical response, it was concluded that the addition of nanosilicate led to a significant enhancement of the storage modulus (40%–50%) at temperatures below ambient which was more pronounced up to filler contents of 5 wt%. Further increase of the filler content led to more conventional composites, which hindered the reinforcing ability of the silicates. The LPDE reinforced with mont-

TABLE 2. Comparison of the calculated E' of the LDPE-OLp and LDPE-OMt composites with the measured ones at –120°C.

W_f (%)	W_m (%)	LDPE-OLp E'_c (GPa) (calculated)	LDPE-OLp E'_c (GPa) (measured)	LDPE-OMt E'_c (GPa) (calculated)	LDPE-OMt E'_c (GPa) (measured)
2	98	3.64	3.82	4.42	4.17
5	95	3.86	4.46	5.86	5.00
10	90	4.25	4.64	8.40	4.58

E'_c: Storage modulus of the composite.

morillonite had better performance in the whole temperature range than those with laponite. It was suggested that the relatively high aspect ratio montomorillonite clay platelets can induce superior dynamic mechanical properties to the LDPE polymer compared to lower aspect ratio clay (laponite) due to higher active surface area and preferential orientation of longer platelets into the testing direction. XRD results in conjunction with an approach to estimate the degree of exfoliation/intercalation using conventional composite theories support the aforementioned findings.

ACKNOWLEDGMENT

The authors thank the Ring of the Laboratory Units and Centers of the U.I. for the XRD and DMA experiments.

REFERENCES

1. J.W. Gilman, *Appl. Clay Sci.*, **15**, 31 (1999).
2. M. Alexandre and P. Dubois, *Mater. Sci. Eng. R: Rep.*, **28**, 1–2 (2000).
3. M. Alexandre, P. Dubois, T. Sun, J.M. Garces, and R. Jerome, *Polymer*, **43**, 8 (2002).
4. S. Sinha Ray and M. Okamoto, *Prog. Polym. Sci*, **28**, 11 (2003).
5. S. Wang, Y. Hu, Q. Zhongkai, Z. Wang, Z. Chen, and W. Fan, *Mater. Lett.*, **57**, 18 (2002).
6. S. Arunvisut, S. Phummanee, and A. Somwangthanaroj, *J. Appl. Polym. Sci.*, **106**, 4 (2007).
7. R.K. Gupta and S.N. Bhattacharya, *Indian Chem. Eng.*, **50**, 3 (2008).
8. C. Broekaert, S. Peeterbroeck, S. Benali, F. Monteverde, L. Bonnaud, M. Alexandre, and P. Dubois, *Eur. Polym. J.*, **43**, 10 (2007).
9. M.J. Solomon, A.S. Almusallam, K.F Seefeldt, A. Somwangthanaroj, and P. Varadan, *Macromolecules*, **34**, 6 (2001).
10. R. Krishnamoorti and A.S. Silva, *Rheological Properties of Polymer-Layered Silicate Nanocomposites*, Hoboken, Wiley, (2000).
11. P.R.D. Kint, G. Seeley, M. Gio-Batta, and A.N. Burgess, *J. Macromol. Sci. B: Phys*, **44**, 6 (2005).
12. E.W. Gacitua, A.A. Ballerini, and J. Zhang, *Cienc. y tecnol.*, **7**, 3 (2005).
13. T.G. Gopakumar, J.A. Lee, M. Kontopoulou, and J.S. Parent, *Polymers*, **43**, 20 (2002).
14. A.A. Bafna, Polyethylene-clay nanocomposites: Processing–strucutre–property relationship. Dissertation, University of Cincinnati (2004).
15. G. Malucelli, S. Ronchetti, N. Lak, A. Priola, N. Tzankova Dintcheva, and F.P. La Mantia, *Eur. Polym J.*, **43**, 2 (2007).
16. B. Baghaei, S.H. Jafari, H.A. Khonakdar, I. Rezaeian, L. As'habi, and S. Ahmadian, *Polym. Bull.*, **62**, 2 (2009).
17. K.H. Wang, M.H. Choi, C.M. Koo, Y.S. Choi, and I.J. Chung, *Polymers*, **42**, 24 (2001).
18. K.H. Wang, M.H. Choi, C.M. Koo, M. Xu, I.J. Chung, M.C. Jang , S.W. Choi, and H.H. Song, *J. Polym. Sci. B: Polym. Phys.*, **40**, 14 (2002).
19. G. Liang, J. Xu, S. Bao, and W. Xu, *J. Appl. Polym. Sci.*, **91**, 6 (2004).
20. K.J. Hwang, J-W. Park, I. Kim, and C-S. Ha, *Macromol. Res.*, **14**, 2 (2006).
21. M.M. Reddy, R.K. Gupta, S.N. Bhattacharya, and R. Parthasarathy, *Korea-Aust. Rheol. J.*, **19**, 3 (2007).
22. Y. Kojima, A. Usuki, M. Kawasumi, A. Okada, T. Kurauchi, and O. Kamigaito, *J. Polym. Sci. A: Polym. Chem.*, **31**, 4 (1993).
23. P.B. Messersmith and E.P. Giannelis, *J. Polym. Sci. A: Polym. Chem.*, **33**, 7 (1995).
24. A. Akelah and A. Moet, *J. Mater. Sci.*, **31**, 13 (1996).
25. J. Tudor, L. Willington, D. O'Hare, and B. Royan, *Chem. Commun.*, 17 (1996).
26. J.S. Bergman, H. Chen, E.P. Giannelis, M.G. Thomas, and G.W. Coates, *Chem. Commun.*, 21 (1999).
27. A. Pegoretti, A. Dorigato, and A. Penati, *Express Polym. Lett.*, **1**, 3 (2007).
28. J.H. Lee, D. Jung, C.E. Hong, K.Y. Rhee, and S.G. Advani, *Compos. Sci. Technol.*, **65**, 13 (2005).
29. A. Giannakas, P. Xidas, K.S. Triantafyllidis, A. Katsoulidis, and A. Ladavos, *J. Appl. Polym. Sci.*, **114**, 1 (2009).
30. A.G. Supri, H. Salmah, and K. Hazwan, *Malaysian Polym. J.*, **3**, 2 (2008).
31. H.M. Yang and Q. Zheng, *Chin. Chem. Lett.*, **15**, 1, (2004).
32. F.P. La Mantia, N.T. Dintcheva, G. Filippone, and D. Acierno, *J. Appl. Polym. Sci.*, **102**, 5 (2006).
33. R. Krishnamoorti and K. Yurekli, *Curr. Opin. Colloid Interface Sci.*, **6**, 5–6 (2001).
34. J. Ren, A.S. Silva, and R. Krishnamoorti, *Macromolecules*, **33**, 10 (2000).
35. K-H. Nitta and A. Tanaka, *Polymers*, **42**, 3 (2001).
36. Y. Ohta and H. Yasuda, *J. Polym. Sci. B: Polym. Phys.*, **32**, 13 (1994).
37. H.A. Khonakdar, U. Wagenknecht, S.H. Jafari, R. Hässler, and H. Eslami, *Adv. Polym. Technol.*, **23**, 4 (2004).
38. S. Rezanejad and M. Kokabi, *Eur. Polym. J.*, **43**, 7 (2007).
39. B. Chen and J.R.G. Evans, *Scr. Mater.*, **54**, 9 (2006).
40. M. Joulazadeh and A.H. Navarchian, *Polym. Adv. Technol.*, **22**, 12 (2010).
41. A. Montazeri, N. Montazeri, K. Pourshamsian, and A. Tcharkhtchi, *Int. J. Polym. Anal. Chem.*, **16**, 7 (2011).
42. N-H. Tai, M-K. Yeh, and T-H. Peng, *Compos. B: Eng.*, **39**, 6 (2008).
43. Y.Q. Rao and J.M. Pochan, *Macromolecules*, **40**, 2 (2007).
44. J.C. Halpin and N.J. Pagano, *J. Compos. Mater.*, **3**, 4 (1969).
45. J.C. Halpin and J.L. Kardos, *Polym. Eng. Sci.*, **16**, 5 (1976).
46. L. Chunsheng and M. Yiu-Wing, *Compos. Sci. Technol.* **67**, 14 (2007).